molecular pharmaceutics

articles

# Relevance of Biophysical Interactions of Nanoparticles with a Model Membrane in Predicting Cellular Uptake: Study with TAT Peptide-Conjugated Nanoparticles

**Chiranjeevi Peetla, Kavitha S. Rao, and Vinod Labhasetwar***

*Department of Biomedical Engineering, Lerner Research Institute, Cleveland Clinic, Cleveland, Ohio 44195*

Received January 13, 2009; Revised Manuscript Received February 14, 2009; Accepted February 25, 2009

**Abstract:** The aim of the study was to test the hypothesis that the biophysical interactions of the trans-activating transcriptor (TAT) peptide-conjugated nanoparticles (NPs) with a model cell membrane could predict the cellular uptake of the encapsulated therapeutic agent. To test the above hypothesis, the biophysical interactions of ritonavir-loaded poly(L-lactide) nanoparticles (RNPs), conjugated to either a TAT peptide (TAT-RNPs) or a scrambled TAT peptide (sc-TAT-RNPs), were studied with an endothelial cell model membrane (EMM) using a Langmuir film balance, and the corresponding human vascular endothelial cells (HUVECs) were used to study the uptake of the encapsulated therapeutic. Biophysical interactions were determined from the changes in surface pressure (SP) of the EMM as a function of time following interaction with NPs, and the compression isotherm ($\pi-$A) of the EMM lipid mixture in the presence of NPs. In addition, the EMMs were transferred onto a silicon substrate following interactions with NPs using the Langmuir−Schaeffer (LS) technique. The transferred LS films were imaged by atomic force microscopy (AFM) to determine the changes in lipid morphology and to characterize the NP−membrane interactions. TAT-RNPs showed an increase in SP of the EMM, which was dependent upon the amount of the peptide bound to NPs and the concentration of NPs, whereas sc-TAT-RNPs and RNPs did not show any significant change in SP. The isotherm experiment showed a shift toward higher mean molecular area (mmA) in the presence of TAT-RNPs, indicating their interactions with the lipids of the EMM, whereas sc-TAT-RNPs and RNPs did not show any significant change. The AFM images showed condensation of the lipids following interaction with TAT-RNPs, indicating their penetration into the EMM, whereas RNPs did not cause any change. Surface analysis and 3-D AFM images of the EMM further confirmed penetration of TAT-RNPs into the EMM, whereas RNPs were seen anchored loosely to the membrane, and were significantly less in number than TAT-RNPs. We speculate that hydrophobic tyrosine of the TAT that forms the NP−interface drives the initial interactions of TAT-RNPs with the EMM, followed by electrostatic interactions with the anionic phospholipids of the membrane. In the case of sc-TAT-RNPs, hydrophilic arginine forms the NP−interface that does not interact with the EMM, despite having the similar cationic charge on these NPs as TAT-RNPs. TAT peptide alone did not show any change in SP, suggesting that the interaction occurs when the peptide is conjugated to a carrier system. HUVECs showed higher uptake of the drug with TAT-RNPs as compared to that with sc-TAT-RNPs or RNPs, suggesting that the biophysical interactions of NPs with cell membrane lipids play a role in cellular internalization of NPs. In conclusion, TAT peptide sequence and the amount of TAT conjugated to NPs significantly affect the biophysical interactions of NPs with the EMM, and these interactions correlate with the cellular delivery of the encapsulated drug. Biophysical interactions with a model membrane thus could be effectively used in developing efficient functionalized nanocarrier systems for drug delivery applications.

**Keywords:** Drug delivery; nanocarriers; cell-penetrating peptides; polymers; nanotoxicity

## Introduction

Intracellular delivery or transport of certain biotherapeutic agents across biological barriers (e.g., blood−brain barrier, BBB) is hampered primarily due to the lipophilic nature of the cell membrane.[1] This barrier to drug transport could also be posed due to the physiochemical properties of certain therapeutic agents, such as their high molecular weight, or

* Author for correspondence: Vinod Labhasetwar, Ph.D., Department of Biomedical Engineering/ND-20, Cleveland Clinic, 9500 Euclid Avenue, Cleveland, OH 44195. Tel: 216/445-9364. Fax 216 /444-9198. E-mail: labhasv@ccf.org.

(1) Deshayes, S.; Simeoni, F.; Morris, M. C.; Divita, G.; Heitz, F. Peptide-mediated delivery of nucleic acids into mammalian cells. *Methods Mol. Biol.* **2007**, *386*, 299–308.

10.1021/mp900011h CCC: $40.75 
Published on Web 02/26/2009

they could act as a substrate for the efflux transporters present on the cell membrane (e.g., P-glycoprotein, P-gp).[1,2] Nanocarriers such as liposomes, dendrimers, and nanoparticles (NPs) have been widely used as delivery systems for various therapeutic agents to overcome these cellular barriers, but their efficacy to deliver drugs intracellularly is limited due to inefficient interactions of NPs with the cell membranes[3] and their uptake process.[4] To improve cellular uptake and transport of these carrier systems, efforts have been directed toward functionalizing their surface with peptides, antibodies, or cationic surfactants.[5,6]

Functionalization of nanocarriers with cell-penetrating peptides (CPPs) is one of the successful strategies that has been developed to overcome the low cellular permeability of the encapsulated agents. Antennapedia,[7] transportan,[8,9] and HIV-1 TAT (trans-activating transcriptor) peptide[10−12] are examples of different CPPs with membrane-translocating properties that are being used to transport different cargoes. CPP-mediated cellular delivery has been demonstrated to occur rapidly across various cell types, and specific integral protein transduction domains (PTDs) of the CPPs are responsible for their cellular uptake. Among the different CPPs with membrane-translocating properties, the HIV-1 TAT peptide and its derivatives are highly utilized for cellular delivery.[13] Christian et al. demonstrated that TAT peptide conjugated to near-infrared (NIR) emissive polymersomes are more efficiently taken up by the dendritic cells (DCs) *in vitro* than unconjugated polymersomes. It is suggested that the labeled DCs could be imaged by NIR fluorescence based imaging to study their trafficking in the body.[14]

The PTD of TAT peptide consists of an 11-amino acid sequence with at least six arginine and two lysine residues, thereby making the peptide highly cationic.[15−17] Significantly different pathways, such as clathrin-dependent endocytosis, lipid raft-dependent macropinocytosis, and direct movement through lipid bilayers (nonendocytic pathway), have been proposed to explain their internalization.[16,18,19] In this study, we were interested in understanding the biophysical interactions of TAT peptide-conjugated NPs with a model cell membrane, and to determine how these interactions correlate with cellular uptake of the encapsulated agent. We tested the effects of the TAT peptide sequence and the amount of peptide conjugated to NPs on biophysical interactions with an endothelial cell model membrane (EMM), and the corresponding human vascular endothelial cells (HUVECs) were used to determine the uptake of the encapsulated therapeutic. Ritonavir was chosen as a model drug since it possesses limited cellular permeability and transport, attributed mainly to its P-gp-mediated efflux.[20] Our results demonstrate that the TAT peptide sequence and the amount of TAT conjugated to NPs significantly affect the biophysical

(2) Deshayes, S.; Morris, M.; Heitz, F.; Divita, G. Delivery of proteins and nucleic acids using a non-covalent peptide-based strategy. *Adv. Drug Delivery Rev.* **2008**, *60*, 537–547.
(3) Vasir, J. K.; Labhasetwar, V. Quantification of the force of nanoparticle-cell membrane interactions and its influence on intracellular trafficking of nanoparticles. *Biomaterials* **2008**, *29*, 4244–4252.
(4) Panyam, J.; Labhasetwar, V. Dynamics of endocytosis and exocytosis of poly(D, L-lactide-co-glycolide) nanoparticles in vascular smooth muscle cells. *Pharm. Res.* **2003**, *20*, 212–220.
(5) Trehin, R.; Merkle, H. P. Chances and pitfalls of cell penetrating peptides for cellular drug delivery. *Eur. J. Pharm. Biopharm.* **2004**, *58*, 209–223.
(6) Yezhelyev, M.; Yacoub, R.; O'Regan, R. Inorganic nanoparticles for predictive oncology of breast cancer. *Nanomedicine* **2009**, *4*, 83–103.
(7) Derossi, D.; Calvet, S.; Trembleau, A.; Brunissen, A.; Chassaing, G.; Prochiantz, A. Cell internalization of the third helix of the antennapedia homeodomain is receptor-independent. *J. Biol. Chem.* **1996**, *271*, 18188–18193.
(8) Soomets, U.; Lindgren, M.; Gallet, X.; Hallbrink, M.; Elmquist, A.; Balaspiri, L.; Zorko, M.; Pooga, M.; Brasseur, R.; Langel, U. Deletion analogues of transportan. *Biochim. Biophys. Acta, Biomembr.* **2000**, *1467*, 165–176.
(9) Yandek, L. E.; Pokorny, A.; Floren, A.; Knoelke, K.; Langel, U.; Almeida, P. F. F. Mechanism of the cell-penetrating peptide transportan 10 permeation of lipid bilayers. *Biophys. J.* **2007**, *92*, 2434–2444.
(10) Ziegler, A.; Blatter, X. L.; Seelig, A.; Seelig, J. Protein transduction domains of HIV-1 and SIV TAT interact with charged lipid vesicles. Binding mechanism and thermodynamic analysis. *Biochemistry* **2003**, *42*, 9185–9194.
(11) Eum, W. S.; Jang, S. H.; Kim, D. W.; Choi, H. S.; Choi, S. H.; Kim, S. Y.; An, J. J.; Lee, S. H.; Han, K.; Kang, J. H.; Kang, T. C.; Won, M. H.; Cho, Y. J.; Choi, J. H.; Kim, T. Y.; Park, J.; Choi, S. Y. Enhanced transduction of Cu, Zn-superoxide dismutase with HIV-1 Tat protein transduction domains at both termini. *Mol. Cells* **2005**, *19*, 191–197.
(12) Al-Taei, S.; Penning, N. A.; Simpson, J. C.; Futaki, S.; Takeuchi, T.; Nakase, I.; Jones, A. T. Intracellular traffic and fate of protein transduction domains HIV-1 TAT peptide and octaarginine. Implications for their utilization as drug delivery vectors. *Bioconjugate Chem.* **2006**, *17*, 90–100.
(13) Chen, B.; Liu, Q.; Zhang, Y.; Xu, L.; Fang, X. Transmembrane delivery of the cell-penetrating peptide conjugated semiconductor quantum dots. *Langmuir* **2008**, *24*, 11866–11871.
(14) Christian, N. A.; Milone, M. C.; Ranka, S. S.; Li, G.; Frail, P. R.; Davis, K. P.; Bates, F. S.; Therien, M. J.; Ghoroghchian, P. P.; June, C. H.; Hammer, D. A. Tat-functionalized near-infrared emissive polymersomes for dendritic cell labeling. *Bioconjugate Chem.* **2007**, *18*, 31–40.
(15) Vives, E.; Brodin, P.; Lebleu, B. A truncated HIV-1 Tat protein basic domain rapidly translocates through the plasma membrane and accumulates in the cell nucleus. *J. Biol. Chem.* **1997**, *272*, 16010–16017.
(16) Hallbrink, M.; Floren, A.; Elmquist, A.; Pooga, M.; Bartfai, T.; Langel, U. Cargo delivery kinetics of cell-penetrating peptides. *Biochim. Biophys. Acta* **2001**, *1515*, 101–109.
(17) Torchilin, V. P. Tat peptide-mediated intracellular delivery of pharmaceutical nanocarriers. *Adv. Drug Delivery Rev.* **2008**, *60*, 548–558.
(18) Vives, E. Cellular uptake [correction of utake] of the Tat peptide: an endocytosis mechanism following ionic interactions. *J. Mol. Recognit.* **2003**, *16*, 265–271.
(19) Zorko, M.; Langel, U. Cell-penetrating peptides: mechanism and kinetics of cargo delivery. *Adv. Drug Delivery Rev.* **2005**, *57*, 529–545.
(20) Alsenz, J.; Steffen, H.; Alex, R. Active apical secretory efflux of the HIV protease inhibitors saquinavir and ritonavir in Caco-2 cell monolayers. *Pharm. Res.* **1998**, *15*, 423–428.

***Table 1.*** Physicochemical Properties of TAT-Conjugated Nanoparticles (NPs) and Their Effect on the Change in Surface Pressure (SP) of the Endothelial Model Cell Membrane (EMM)

| formulation | TAT peptide added for conjugation[a] ($\mu$g) | TAT molecules conjugated/NP | mean NP size in nm (PI) | $\zeta$-potential (mV) | $\Delta$SP[b] (mN/m) |
|---|---|---|---|---|---|
| RNPs (without epoxy activation) | | | 234 (0.04) | $-19.3 \pm 0.3$ | 0.9 |
| $TAT_{20}$-RNPs | 20 | 750 | 321 (0.04) | $2.0 \pm 0.2$ | 3.9 |
| $TAT_{200}$-RNPs | 200 | 2042 | 338 (0.23) | $3.5 \pm 0.2$ | 5.8 |
| $TAT_{500}$-RNPs | 500 | 3980 | 355 (0.20) | $20.3 \pm 0.7$ | 9.0 |
| sc-$TAT_{200}$-RNPs | 200 | 2531 | 310 (0.18) | $5.0 \pm 0.5$ | 0.5 |
| ritonavir alone | | | | | 0.0 |
| TAT peptide alone | | | | | 0.0 |
| sc-TAT peptide alone | | | | | 0.0 |

[a] Initial amount of TAT peptide added to 60 mg of ritonavir-loaded nanoparticles during conjugation. Numbers in subscripts for different formulations of conjugated NPs indicate the initial amount of TAT peptide added for conjugation. RNPs: Ritonavir-loaded NPs. TAT-RNPs: TAT peptide-conjugated RNPs. sc-TAT-RNPs: scrambled TAT peptide-conjugated RNPs. PI: polydispersity index. [b] Change in SP of the EMM with respect to injection of water.

interactions of NPs with the EMM, and these interactions correlate with the cellular delivery of the encapsulated drug.

## Materials and Methods

Poly(L-lactide) (PLA, inherent viscosity = 0.4 dL/g, molecular weight 40,000) was purchased from Durect Corporation (Pelham, AL). Ritonavir (Toronto Research Chemicals, Inc., North York, Ontario, Canada) and tritium-labeled ($^3$H) ritonavir (Moravek Biochemicals, Brea, CA) were purchased. TAT peptide of the sequence Tyr-Gly-Arg-$(Lys)_2$-$(Arg)_2$-Gln-$(Arg)_3$ (molecular weight 1917) was custom synthesized by Invitrogen Corporation (Carlsbad, CA) while the scrambled peptide of the sequence Arg-Lys-Arg-Gly-Arg-Lys-Arg-Tyr-Arg-Gln-Arg was synthesized in-house at the Molecular Biotechnology Core Facility. Denacol EX-521 (pentaepoxy, molecular weight 742) was a gift from Nagase Chemicals Ltd. (Tokyo, Japan). Scintillation cocktail, ScintiVerse, was obtained from PerkinElmer, Inc. (Waltham, MA). Zinc tetrahydrofluoroborate hydrate, poly(vinyl alcohol) (PVA, average molecular weight 30,000−70,000), dextran and boric acid were purchased from Sigma Chemical Co. (St. Louis, MO).

Lipids, 1,2-dipalmitoyl-*sn*-glycero-3-phosphocholine (DPPC), 1,2-dipalmitoyl-*sn* -glycero-3-phospho- L-serine (DPPS), L-α-phosphatidylinositol (PI), sphingomyelin (SM), and cardiolipin (CL) were purchased from Avanti Polar Lipids, Inc. (Alabaster, AL). HPLC grade chloroform, methanol and ethanol were obtained from Fisher Scientific (Fair Lawn, NJ). Dulbecco's phosphate buffered saline (D-PBS) was obtained from in-house Central Cell Services' Media Laboratory. Ammonium hydroxide ($NH_4OH$) and hydrofluoric acid (HF) were purchased from Acros Organics (Fair Lawn, NJ), and hydrogen peroxide ($H_2O_2$) was purchased from Fisher Scientific. Deionized water with 18.2 MΩ·cm resistivity, collected from the Super Q water system (Millipore Corporation, Billerica, MA), was used in all the experiments.

Endothelial basal medium (EBM), growth factors (bovine brain extract with heparin), human endothelial growth factor (hEGF), hydrocortisone, GA-1000 (gentamicin and amphotericin B), and fetal bovine serum (FBS) were purchased from Lonza (Walkersville, MD).

**Formulation of NPs.** NPs containing unlabeled ritonavir were used for the biophysical studies, while NPs containing $^3$H-ritonavir were used for the uptake studies in HUVECs. First, ritonavir-loaded NPs (RNPs) were formulated using an emulsion−solvent evaporation technique and then conjugated to either TAT peptide or scrambled TAT (sc-TAT) peptide as described in our previous study (see details in Supporting Information).[21] Briefly, the conjugation of peptides first involved surface activation of the formulated NPs by the epoxy-linker Denacol in the presence of catalyst, zinc tetrahydrofluoroborate hydrate. The surface-activated NPs were then incubated with the desired amount of TAT or sc-TAT peptide (Table 1). NPs were incubated with three different initial amounts of TAT peptide: 20 $\mu$g, 200 $\mu$g or 500 $\mu$g; or with 200 $\mu$g of sc-TAT peptide. These formulations were described as $TAT_{20}$-, $TAT_{200}$-, $TAT_{500}$-, and sc-$TAT_{200}$-RNPs, respectively, with the numbers in the subscripts representing the amount of peptide used during the conjugation reaction. Fluorescein-conjugated TAT peptide (Invitrogen Corporation) was used for quantifying the amount of unconjugated TAT peptide by fluorescence spectroscopy (LS55, PerkinElmer, Inc.) at $\lambda_{ex} = 488$ nm, $\lambda_{em} = 520$ nm. The amount of unconjugated peptide was then subtracted from the initial amount of the peptide added to the reaction mixture to obtain the amount of peptide conjugated to NPs. Number of peptide molecules conjugated to per NP was calculated as per the calculations described in our previous study.[21]

**Physical Characterization of NPs.** A 50 $\mu$L aliquot of each NP suspension (5 mg/mL) was diluted to 3 mL with water. The mean hydrodynamic size was measured by a dynamic light scattering technique, and $\zeta$-potential was determined with a phase analysis light scattering technique (PSS/NICOMP 380/ZLS, Particle Sizing Systems, Santa Barbara, CA). For particle size analysis by transmission electron microscopy (TEM), a drop of NP suspension was placed on a Formvar-coated copper TEM grid, air-dried, counterstained with a 2% (w/v) aqueous solution of uranyl

(21) Rao, K. S.; Reddy, M. K.; Horning, J. L.; Labhasetwar, V. TAT-conjugated nanoparticles for the CNS delivery of anti-HIV drugs. *Biomaterials* **2008**, *29*, 4429–4438.

acetate (Sigma Chemical Co.), and air-dried again prior to visualization using a Philips CM12 electron microscope (FEI Company, Hillsboro, OR). The NIH ImageJ software was used to calculate mean particle size from the TEM photomicrographs.

**Endothelial Cell Model Membrane (EMM).** The EMM is a monolayer of a lipid mixture, which was compressed to a surface pressure (SP) of 30 mN/m on the D-PBS surface using the Langmuir−Blodgett instrument (KSV Inc., Helsinki, Finland). The lipid mixture contained different lipids with a headgroup composition similar to that found in the native artery's endothelial cell membrane (see details in Supporting Information).[22,23]

**Interaction of NPs with EMM.** A 500 $\mu$L aliquot of NP suspension (5 mg/mL concentration) was injected below the surface of the EMM through the injection port over a period of 30 s using a Hamilton digital microsyringe (Hamilton, Reno, NV), and the change in SP was measured immediately. Precaution was taken to ensure that the injection did not disturb the membrane. Control experiments (free ritonavir, free TAT peptide, and free sc-TAT peptide) were carried out to ensure that the changes observed in SP of the EMM were due to interaction of the conjugated NPs. Based on the release data, 15 $\mu$g of ritonavir is released within 30 min from 2.5 mg of ritonavir-encapsulated NPs. Therefore, the free drug control experiment involved 500 $\mu$L of aqueous solution containing 15 $\mu$g of ritonavir. A stock solution of drug in ethanol was appropriately diluted in water to achieve the above concentration. The amount of ethanol used in drug solution was shown to have no effect on the SP of the EMM. It was determined that 50 $\mu$g of TAT peptide or sc-TAT peptide was bound to 2.5 mg of $TAT_{200}$-RNPs. Therefore, the control experiments with free TAT peptide or free sc-TAT peptide were carried out with the above amount of peptide dissolved in 500 $\mu$L of water. Water alone was also used as a control since suspension of NPs and peptide solutions were prepared in water. Changes in SP of the EMM with respect to time were recorded immediately at a constant mean molecular area (mmA) for a period of 20 min.

**Effect of NP Concentration on Changes in SP of EMM.** To determine the effect of NP concentration on SP of the EMM, a different volume of NP suspension was injected into the trough with a corresponding volume of water injected as a control. The concentration of NPs was calculated from the trough volume (50 mL) and the weight of NPs that was injected. For instance, a 500 $\mu$L injection of 5 mg/mL NP suspension in 50 mL of buffer in the trough gives a NP concentration of 50 $\mu$g/mL.

**Effect of NPs on $\pi-A$ isotherm of Endothelial Lipid Mixture.** These experiments were performed to investigate the penetratability of NPs into the EMM. The EMM lipid mixture was spread at the low SP of 0 mN/m. A 500 $\mu$L aliquot of the NP suspension (5 mg/mL concentration) was injected below the lipid mixture; NPs were allowed to interact for 20 min with the lipid mixture and then compressed at the rate of 3 mm/min until the film collapsed.

**Langmuir−Schaeffer (LS) Film Transfer for AFM Imaging.** For this experiment, the EMM was formed on the buffer surface, and then NPs were injected below the EMM as described above. NPs were allowed to interact with the EMM for 20 min prior to its transfer onto the substrate using the Langmuir−Schaeffer (LS) technique (see details in Supporting Information). The transferred LS films were subsequently allowed to dry in air for at least 24 h in a desiccator at room temperature prior to AFM imaging.

**AFM of LS Films.** Surface morphology of the LS films before and following interaction with NPs was studied with a Bioscope II atomic force microscope (Veeco Metrology, Inc., Santa Barbara, CA). AFM images were collected in tapping mode using a silicon cantilever (Veeco Metrology) of 125 $\mu$m in length with a resonance frequency of approximately 325 Hz and a tip radius of 10 nm. The images were captured with a lateral scan frequency of 1−2 Hz and a set point ratio of 0.98. The acquired images were flattened using a second order flattening routine in digital instrument software (Nanoscope version 7.0, Veeco Metrology). The images from three different LB films for each sample were taken to ensure reproducibility.

**Uptake and Cytotoxicity Studies.** HUVECs were seeded in 24-well plates at a seeding density of 30,000 cells per well and were allowed to attach for 24 h, followed by a medium change every other day. Cells were allowed to grow for 4 days, the medium was aspirated, and the cells were washed twice with D-PBS prior to incubation with ritonavir solution (5 $\mu$M) or the equivalent amount of RNPs, TAT-RNPs, or sc-TAT-RNPs for a period of 15, 30, or 60 min at 37 °C. Following incubation, the cells were washed thrice with D-PBS, lysed by the addition of 0.5 mL of trypsin, and then underwent a series of alternating freeze−thaw cycles. The cell lysate obtained thereof (0.4 mL) was analyzed for ritonavir level by a liquid scintillation counter, while the remaining 0.1 mL of the cell lysate was used to estimate protein content by a Bradford protein assay (Bio-Rad, Hercules, CA). A standard plot with different concentrations of drug-loaded NPs was constructed simultaneously under identical conditions to determine the drug levels in cell lysates and the levels were normalized to protein content. Cytotoxicity of different formulations of NPs was determined by a mitogenic (MTS) assay using the Cell Titer 96 $AQ_{ueous}$ Cell Proliferation Assay Kit (Promega Corporation, Madison, WI).

## Results

**Physical Characterization of NPs.** With increasing the amount of the added TAT peptide, the amount of TAT

(22) Leray, C.; Andriamampandry, M.; Gutbier, G.; Cavadenti, J.; KleinSoyer, C.; Gachet, C.; Cazenave, J. P. Quantitative analysis of vitamin E, cholesterol and phospholipid fatty acids in a single aliquot of human platelets and cultured endothelial cells. *J. Chromatogr. B* **1997**, *696*, 33–42.

(23) Peetla, C.; Labhasetwar, V. Biophysical characterization of nanoparticle-endothelial model cell membrane interactions. *Mol. Pharmaceutics* **2008**, *5*, 418–429.

peptide conjugated to NPs also increased; however, with decreasing efficiency as the NP surface became saturated (Table 1). The mean hydrodynamic diameter of unconjugated RNPs was 234 nm, and upon conjugation this increased to >300 nm. The mean particle size measured using TEM was 125 ± 6.3 nm which, for conjugated NPs was 157 ± 8.9 nm (mean ± SEM, $n = \sim 70$). The discrepancy in size between hydrodynamic diameter and that measured using TEM has been attributed to the hydration of the NP associated PVA (PVA is used as an emulsifier, a fraction of which remains associated with NPs even after repeated washing of NPs[24]). Epoxy activation of RNPs prior to conjugation with TAT further contributes toward hydrodynamic diameter. The ζ-potential of the unconjugated RNPs was −19.2 ± 0.3 mV, which became slightly positive at lower concentrations of peptide, but was more cationic at higher peptide concentration. NPs conjugated to TAT or sc-TAT peptide had similar ζ-potentials (Table 1). Ritonavir loading in NPs was 18.6% (w/w).

**Interactions of NPs with EMM.** TAT-RNPs showed almost an exponential increase in SP with time (Figure 1a), and this increase in SP was dependent upon the amount of the peptide conjugated NPs (Table 1). In comparison, RNPs showed an initial marginal increase in SP and then no change with time. On the other hand, sc-TAT-RNPs showed an insignificant increase in SP. There was no change in SP of the EMM observed with water or other controls such as ritonavir in solution, TAT peptide, or sc-TAT peptide (Table 1).

**Effect of NP Concentration on EMM.** The difference in the SP at 20 min was plotted with respect to the concentration of $TAT_{200}$-RNPs (Figure 1b). A polynomial fit of the data depicts that the change in SP of the EMM was linear with an increasing amount (up to 20 μg/mL) of NPs and then reached a plateau at higher concentration (50 μg/mL). The change in SP of the EMM with unconjugated RNPs or sc-TAT-RNPs was negligible even at the highest concentration of NPs tested in this experiment.

**Effect of NPs on the Isotherm of the EMM Phospholipid Mixture.** The shape of the compression isotherm ($\pi - A$) of the EMM phospholipid mixture showed two distinct regions (Figure 2). The lipids of EMM alone showed a gradual increase in SP down to a mean molecular area (mmA) of 100 Å$^2$, and then displayed a small kink at ∼84 Å$^2$ prior to a rapid increase until the membrane collapse occurred at 55 Å$^2$. Both unconjugated RNPs and $TAT_{200}$-RNPs demonstrated an increase in SP from 0 mN/m following injection of NPs and prior to compression of the lipid mixture. With compression, the SP increased gradually to 27 mN/m in the presence of RNPs, followed by a rapid increase until the membrane collapsed at ∼65 Å$^2$. It is interesting to note that the isotherm in the presence of RNPs was almost the same as that of the EMM lipid mixture alone after the SP of 27 mN/m. On the other hand, the isotherm in the presence of $TAT_{200}$-RNPs differed significantly and showed a gradual increase in SP with compression and a shift toward higher mean molecular area until the membrane collapsed at ∼85 Å$^2$. The isotherm in the presence of sc-TAT-RNPs was almost the same as that of the EMM lipid mixture alone (Figure 2).

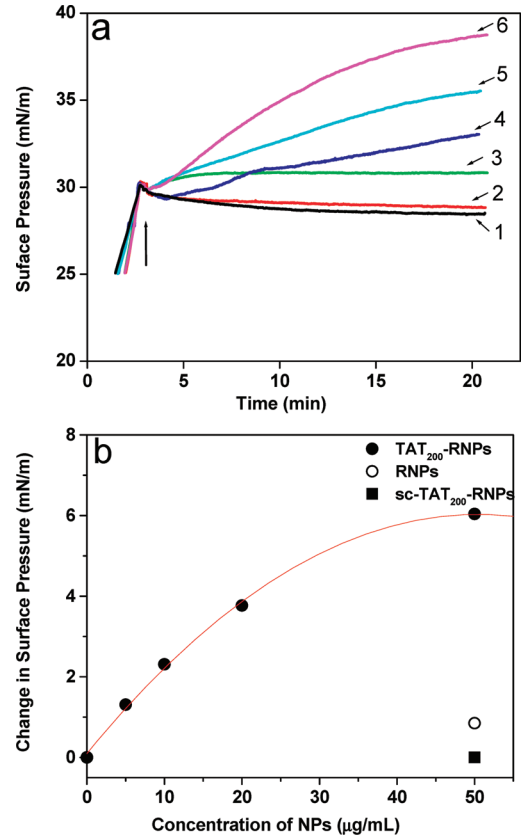


***Figure 1.*** The change in surface pressure (SP) of the endothelial cell model membrane (EMM) following interaction with NPs. (a) Effect of TAT peptide amount and its sequence conjugated to NPs on the change in surface pressure of the EMM. A 500 μL aliquot of NP suspension (5 mg/mL) was injected into the subphase consisting of 50 mL of buffer, and the change in SP of the EMM was recorded immediately with time. Arrow in the figure indicates the point of addition of NPs into subphase. (b) Effect of concentration of unconjugated and conjugated RNPs on the change in SP of the EMM following interaction after 20 min. $TAT_{200}$-RNPs were tested at different concentrations whereas RNPs and sc-$TAT_{200}$-RNPs were tested at the highest concentration used in this experiment. NP concentration in the buffer = 50 μg/mL. Key for (a): 1, EMM without NPs; 2, sc-$TAT_{200}$-RNPs; 3, RNPs; 4, $TAT_{20}$-RNPs; 5, $TAT_{200}$-RNPs; 6, $TAT_{500}$-RNPs.

**AFM Imaging of Langmuir−Schaeffer (LS) Films.** The comparison between the surface morphology of the EMM prior to and after interaction with NPs clearly shows that $TAT_{200}$-RNPs caused condensation of the EMM, but no such changes were seen with RNPs (Figure 3). The phase images of the EMM alone and the EMM following

(24) Sahoo, S. K.; Panyam, J.; Prabha, S.; Labhasetwar, V. Residual polyvinyl alcohol associated with poly (D, L-lactide-co-glycolide) nanoparticles affects their physical properties and cellular uptake. *J. Controlled Release* **2002**, *82*, 105–114.

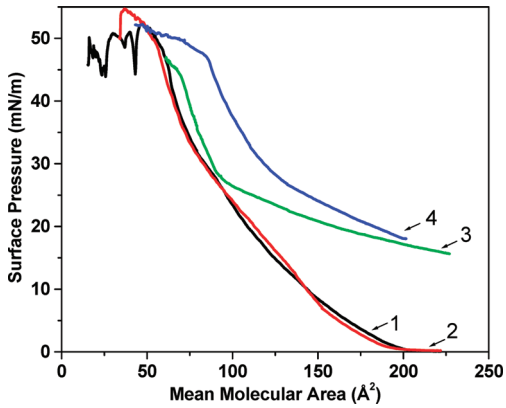


***Figure 2.*** Effect of TAT peptide sequence conjugated to RNPs on the compression isotherm of the endothelial cell model membrane (EMM) lipid mixture. The EMM lipid mixture was spread on the buffer surface at 0 mN/m surface pressure (SP); a suspension of NPs was injected into the subphase prior to compression. NP concentration in the buffer = 50 $\mu$g/mL. Key: 1, EMM without NPs; 2, sc-$TAT_{200}$-RNPs; 3, RNPs; 4, $TAT_{200}$-RNPs.

interaction with RNPs showed bright and dark regions, corresponding to the liquid condensed and liquid order phase of the EMM (Figures 3a and 3b). The phase image of the EMM following interaction with $TAT_{200}$-RNPs, however, demonstrated complete condensation of lipids (Figure 3c). Height images of the EMM following interaction with RNPs and $TAT_{200}$-RNPs (Figures 3b and 3c) showed spherical structures associated with the membrane. The section analysis of the magnified height images of the EMM prior to interaction with NPs (Figure 3d) showed a small height difference in the corresponding liquid condensed and liquid order phases. This is due to the difference in the arrangement of lipids in different phases. Magnified height images and their section analysis, and the corresponding 3-D height images of the EMM following interaction with RNPs (Figure 3e) and $TAT_{200}$-RNPs (Figure 3f) demonstrate that unconjugated RNPs anchor to the EMM while $TAT_{200}$-RNPs were seen embedded in the lipids of the EMM. This is clearly evident from the corresponding section analysis of the LS films where the height range is from 50 to 100 nm for the RNPs-interacted membrane, while that for the TAT-RNPs-interacted membrane is from >10 to 50 nm, with most peaks appearing toward lower height (Figure 3e vs 3f, section analysis and 3-D images). This height is significantly lower than the TEM diameter (~150 nm) of conjugated NPs. The height analysis for the membrane alone is <3 nm (Figure 3d), which is significantly lower than that for the NPs-interacted EMM. Further, the 3-D images clearly show a significantly greater number of TAT-RNPs interacting with the EMM than unconjugated RNPs. The images also show a few aggregates of NPs anchored to the membrane.

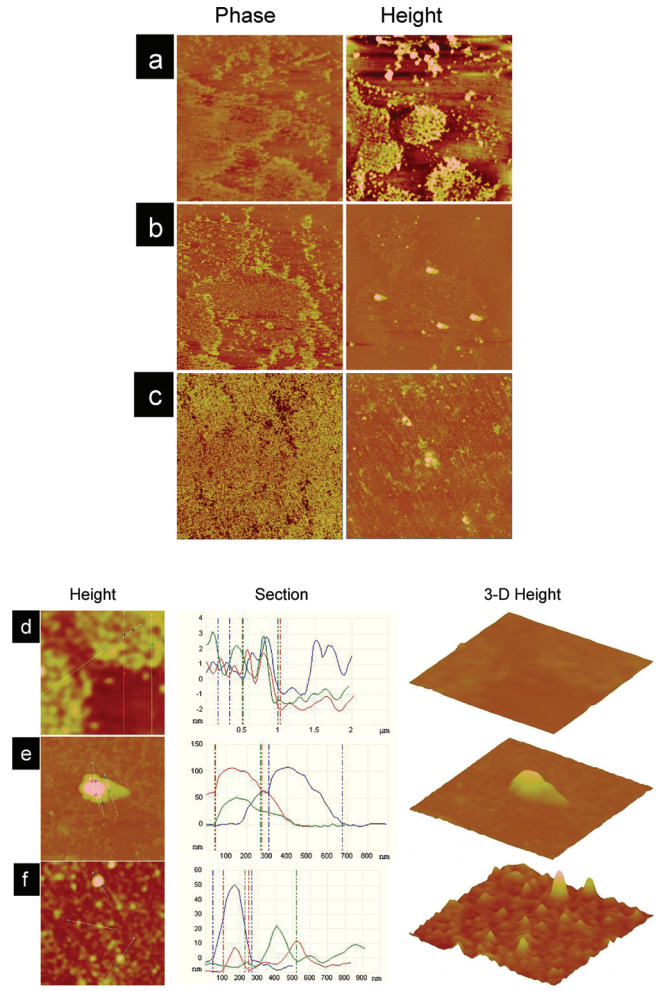


***Figure 3.*** Surface morphology of the endothelial cell model membrane (EMM) following interaction with NPs. Langmuir−Schaeffer films were transferred onto a silicon substrate following interaction with NPs for 20 min, and the imaging was carried out using AFM in tapping mode in air. (a) EMM alone, (b) EMM following interaction with RNPs, and (c) EMM following interaction with $TAT_{200}$-RNPs. The EMM was transferred at the SP 29 mN/m for (a), whereas (b) and (c) were transferred at the SP 31, 36 mN/m, respectively. The corresponding zoom images for (a), (b), (c) are (d), (e), (f). The phase angle scale was 50° for all images. The height scales for the images were a, = 3 nm; b, c, = 150 nm. The section analysis was carried out on the AFM height images across the white lines. The scan size for (a−c) = 10 $\mu$m and (d−f) = 2 $\mu$m.

**Uptake and Cytotoxicity Studies.** Ritonavir uptake in HUVECs was greater with TAT-RNPs as compared to that with RNPs, sc-TAT-RNPs or ritonavir in solution (Figure 4). Further, the drug uptake increased with the increase in the amount of TAT peptide conjugated to NPs. Similar enhancement in the drug uptake was not observed with sc-TAT-RNPs. $TAT_{500}$-RNPs were found to be toxic (Figure 5), and hence the uptake data with these NPs were not considered for comparison. There was no toxicity observed

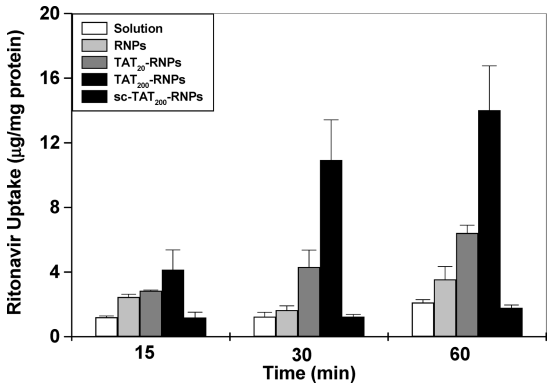


***Figure 4.*** Effect of amount of TAT peptide bound to NP surface and the peptide sequence on uptake of ritonavir in HUVEC cells. Cells ($3 \times 10^4$ cells) were incubated with either ritonavir in solution, or unconjugated and conjugated RNPs (drug concentration = 5 $\mu$M) for different time periods. Data are expressed as mean ± SEM ($n = 3$).

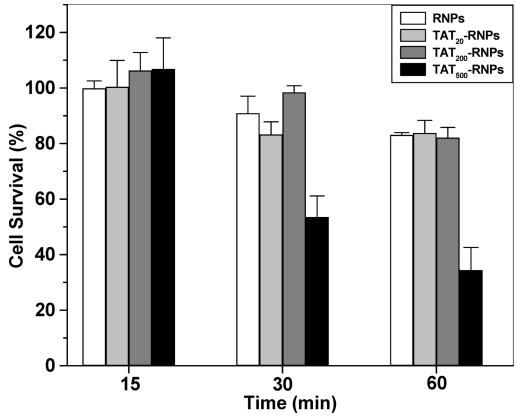


***Figure 5.*** Viability of HUVEC cells incubated with RNPs and TAT-RNPs conjugated to different amount of peptide. HUVEC cells were grown in 96-well plates at a seeding density of 5,000 cells per well until confluency was attained. Cells were then incubated with RNPs or TAT-RNPs and cell viability was assessed using a MTS assay at different time points following incubation. Ritonavir solution or TAT peptide alone did not show any toxicity (data not included in figure). The values represent percentage of viable cells relative to untreated cells. Data are expressed as mean ± SEM ($n = 3$).

with ritonavir solution, RNPs, $TAT_{20}$-, $TAT_{200}$-, or sc-$TAT_{200}$-RNPs.

## Discussion

In this study, we investigated the mechanism of enhanced cellular uptake of an encapsulated drug with TAT-conjugated NPs on the basis of their biophysical interactions with the EMM using a Langmuir balance. Our results demonstrated that the amount of TAT peptide conjugated to NPs, and more importantly the peptide sequence, significantly influence the interaction of conjugated NPs with the EMM. This is evident from (1) the change in SP of the EMM, (2) the compression isotherm ($\pi-A$) of the lipid mixture in the presence of conjugated and unconjugated NPs, and (3) the AFM images of the NPs-interacted LS films. We also observed that the biophysical interactions with the EMM occur only when the peptide is conjugated to NPs and not with the peptide alone. Irrespective of the cellular internalization mechanism of TAT-conjugated NPs, it is believed that a direct contact between the peptide and cell membrane lipids is prerequisite for the successful translocation of NPs across the cell membrane.[25−27] In this regard, biophysical interactions could be critical in understanding the basic parameters in the optimization of nanocarriers for drug delivery applications.

Comparison of the changes in the SP of the EMM due to unconjugated RNPs and TAT-conjugated RNPs clearly demonstrate that the TAT peptide facilitates the interaction of RNPs with the EMM. Additionally, comparison between the interaction of $TAT_{200}$-RNPs and sc-$TAT_{200}$-RNPs with the EMM shows that the NP interactions with the membrane depend on the TAT peptide sequence and not solely on the surface charge of NPs since $TAT_{200}$-RNPs and sc-$TAT_{200}$-RNPs have nearly similar $\zeta$-potential but have different interaction patterns with the EMM. Hyndman et al.[28] have reported that the transfection efficiency of their TAT/liposome/DNA complex was reduced by 50% with a scrambled TAT peptide in A549 human lung carcinoma epithelial cells, signifying the importance of the peptide sequence in effective intracellular delivery of a carrier system.

To ensure that the changes in the SP of the EMM following injection with modified NPs are due to their interaction with the EMM, the changes in SP of buffer alone (without membrane lipids) following injection of NPs were also measured. RNPs and $TAT_{200}$-RNPs exhibited a sharp increase in SP until ~14 mN/m, whereas the SP with sc-$TAT_{200}$-RNPs increased gradually until 5 mN/m and then decreased to 0 mN/m within 20 min (data shown in supplemental section as Figure 1). This suggests that RNPs and $TAT_{200}$-RNPs are surface active while sc-$TAT_{200}$-RNPs do not display the same property. The comparison between the effects of RNPs on buffer with and without membrane clearly suggests that the changes in SP of the EMM following NP injection are due to NP−membrane interactions and not merely due to their intrinsic surface activity. This is because

(25) Al-Taei, S.; Penning, N. A.; Simpson, J. C.; Futaki, S.; Takeuchi, T.; Nakase, I.; Jones, A. T. Intracellular traffic and fate of protein transduction domains HIV-1 TAT peptide and octaarginine. Implications for their utilization as drug delivery vectors. *Bioconjugate Chem.* **2006**, *17*, 90–100.

(26) Ryu, J.; Han, K.; Park, J.; Choi, S. Y. Enhanced uptake of a heterologous protein with an HIV-1 Tat protein transduction domains (PTD) at both termini. *Mol. Cells* **2003**, *16*, 385–391.

(27) Tiriveedhi, V.; Butko, P. A fluorescence spectroscopy study on the interactions of the TAT-PTD peptide with model lipid membranes. *Biochemistry* **2007**, *46*, 3888–3895.

(28) Hyndman, L.; Lemoine, J. L.; Huang, L.; Porteous, D. J.; Boyd, A. C.; Nan, X. HIV-1 Tat protein transduction domain peptide facilitates gene transfer in combination with cationic liposomes. *J. Controlled Release* **2004**, *99*, 435–444.

RNPs and $TAT_{200}$-RNPs showed an almost similar increase in SP of the buffer, but only $TAT_{200}$-RNPs showed an increase in SP of the EMM.

We studied the change in the isotherm of the lipid mixture of the EMM to determine whether the observed change in SP of the EMM was due to penetration by TAT-RNPs or due to electrostatic interactions between phospholipid head groups of the EMM and the cationic arginine or lysine of the TAT peptide conjugated to NPs (Figure 2). In our earlier studies, we have demonstrated an increase in SP of the EMM due to penetration by hydrophobic chains of didodecyl dimethylammonium bromide, a dichained surfactant that was coated onto the surface of polystyrene NPs (130 nm).[29] We also observed an increase in SP due to penetration by smaller sized (20 nm) polystyrene NPs.[23] The results of the isotherm experiment demonstrate that RNPs and $TAT_{200}$-RNPs permeate the lipids of the EMM at lower lipid densities as they demonstrate higher SP than lipid mixture alone. However, RNPs appear to squeeze out of the monolayer as the SP approaches ~30 mN/m, which is the SP of a biological membrane, whereas $TAT_{200}$-RNPs seem to remain within the monolayer. This is evident from the shift toward higher mmA of the EMM in the presence of $TAT_{200}$-RNPs at SP of ~30 mN/m, which was not seen in the presence of RNPs (Figure 2). sc-TAT-RNPs did not alter the EMM isotherm, thus suggesting that they do not have any interactions with the lipids of the EMM.

The difference in the interaction patterns of the $TAT_{200}$-RNPs and sc-$TAT_{200}$-RNPs with the EMM can be attributed to the difference in the arrangement of the amino acid sequence of TAT and sc-TAT peptide. It is surprising to see that scrambling the TAT peptide sequence resulted in such a significant difference in the NP−EMM interactions. RNPs are surface active because of the surface-associated PVA, which is used as an emulsifier during NP formulation. A fraction of PVA remains associated with the NP surface and could not be washed away.[24] Epoxy activation of RNPs did not change the surface-active characteristic of RNPs; however, conjugating them to sc-TAT peptide resulted in their loss of surface activity. This could be because of the hydrophilic nature of sc-TAT peptide[16] as the major amino acids (arginine, lysine, and glutamine) in the peptide are highly hydrophilic as well as highly cationic ($Z = +8$, where $Z$ is valence).[15,30] Therefore, conjugation of sc-TAT peptide could have conferred cationic and hydrophilic properties to RNPs. The ζ-potential analysis demonstrated the change in surface charge of RNPs from −ve to +ve following conjugation to sc-TAT-RNPs. Although conjugation of TAT peptide also showed a similar change in ζ-potential of RNPs, they remained surface active unlike sc-TAT-RNPs. This is possible only if the TAT peptide is conjugated to RNPs in such a way that the nonpolar amino acid, tyrosine is exposed at the NP surface. This could occur only when the conjugation reaction results in covalent bond formation between active epoxy groups and the $-NH_2$ of amino acid, arginine which is present at the other end of the peptide sequence. Based on the observation that TAT-RNPs remain surface active, it is reasonable to state that the conjugation reaction occurs at the arginine end of the peptide sequence. Ren et al.[31] have reported that $-NH_2$ of arginine has greater susceptibility for a bond formation with epoxy groups than other amino acids, thus supporting our assumption. This specific conformation of TAT peptide that exposes the nonpolar tyrosine[32] at the interface imparts surface activity to TAT-RNPs. sc-TAT conjugation does not impart surface activity to RNPs since the amino acid sequence in the peptide begins and ends with arginine, while tyrosine occupy the central portion (Figure 6). This assumption is further supported by the energy minimized conformations of the TAT peptide and sc-TAT peptide as determined using the MM2 force field program (Chemdraw 3D software, Cambridgesoft, Cambridge, MA). In the TAT peptide, the hydrophobic tyrosine is exposed outwardly, whereas in the sc-TAT peptide they occupy the central portion of the

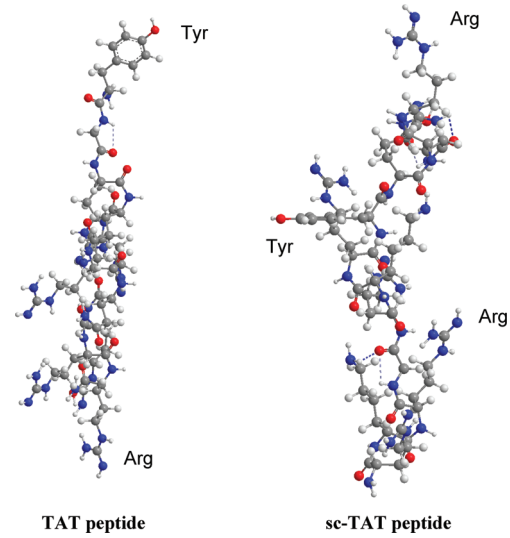


***Figure 6.*** Energy minimized conformation of TAT peptide and sc-TAT peptide. Minimum energy conformations were generated using a MM2 force field. In TAT peptide, tyrosine is at the beginning of the peptide sequence (top), whereas in sc-TAT peptide, it occupies the central portion of the peptide. Tyr-Tyrosine; Arg-Arginine.

(29) Peetla, C.; Labhasetwar, V. Effect of molecular structure of cationic surfactants on biophysical interactions of surfactant-modified nanoparticles with a model membrane and cellular uptake. *Langmuir* **2009**, *25*, 2369–2377.

(30) Brooks, H.; Lebleu, B.; Vives, E. Tat peptide-mediated cellular delivery: back to basics. *Adv. Drug Delivery Rev.* **2005**, *57*, 559–577.

(31) Ren, L.; Tsuru, K.; Hayakawa, S.; Osaka, A. Synthesis and characterization of gelatin-siloxane hybrids derived through sol-gel procedure. *J. Sol-Gel Sci. Technol.* **2001**, *21*, 115–121.

(32) Mathew, C. J.; Wilce, M.-I. A.; Milton, T. W. Heam. Physicochemical basis of amino acid hydrophobicity scales: Evaluation of four new scales of amino acid hydrophobicity coefficients derived from RP-HPLC of peptides. *Anal. Chem.* **1995**, *67*, 1210–1295.

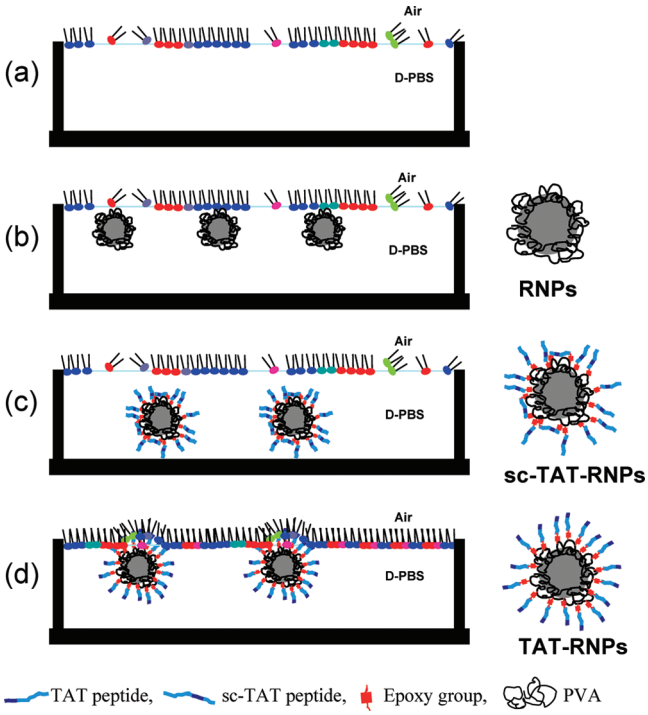


***Figure 7.*** Schematic representation of the interaction of unconjugated, TAT peptide, and sc-TAT peptide conjugated RNPs with the EMM. (a) EMM alone, (b) EMM interacting with RNPs, (c) EMM interacting with sc-TAT-RNPs, and (d) EMM interacting with TAT-RNPs.

peptide (Figure 6). Conjugation can occur at both the ends of the amino acid sequence of sc-TAT peptide, thereby rendering tyrosine unavailable at the interface of NPs. Since TAT-RNPs are surface active, they can come to the interface and interact with the anionic phospholipids in the EMM. On the other hand, sc-TAT-RNPs do not come to the interface because of their lack of surface activity; hence they do not interact with the anionic phospholipids of the EMM despite having a similar $\zeta$-potential as TAT-RNPs (Figure 7). Free TAT peptide as a single chain molecule is hydrophilic and therefore has no surface active property to interact with the EMM. Lack of interaction of free TAT peptide has been reported previously in model membrane studies[33,34] and also in cell culture, where even at high concentration (100 $\mu$m), free TAT peptide did not show plasma membrane perturbation.[16]

Wimley et al.[35,36] have reported hydrophocity of 20 natural amino acids based on their free energy ($\Delta G$) values required for the transfer from water to palmitoyloeoyl phosphatidylcholine bilayer interface (wif). The lower free energy, $\Delta G_{(wif)}$, for tyrosine ($-0.94 \pm 0.06$) in comparison to arginine ($+0.81 \pm 0.11$) indicates that tyrosine has greater propensity to partitioning into the lipid interface than arginine. This supports our assumption that the tyrosine of the conjugated TAT drives the initial interaction of NPs with the lipids of the EMM and the lack of interactions of sc-TAT peptide conjugated NPs. Since multiple molecules of TAT peptide are conjugated to NPs, more hydrophobic chains of tyrosine are exposed at the NP−interface for interaction with the EMM. This also explains the increase in interaction with increased amount of TAT peptide bound to NPs (Figure 1a). Several other studies have signified the role of hydrophobic interactions with cell membrane lipids.[37−39] Wender et al. observed increased cellular uptake of arginine homopolymer upon increasing its hydrophobicity by variation of the methylene content of the side chain of h-amino acids of arginine.[40] Futaki et al.[41] and Chen et al.[42] showed that attachment of hydrophobic group at the N-terminal end of the TAT peptide leads to increased cellular uptake of the conjugates. Based on our studies and others, we speculate that a highly charged peptide with properly placed hydrophobic amino acids should have a better interaction with cell membrane than the one with hydrophilic amino acids. However, it would also depend upon the conformation of the peptide and its anchoring on NPs so that the hydrophobic

(33) Dennison, S. R.; Baker, R. D.; Nicholl, I. D.; Phoenix, D. A. Interactions of cell penetrating peptide Tat with model membranes: A biophysical study. *Biochem. Biophys. Res. Commun.* **2007**, *363*, 178–182.

(34) Nagy, I. B.; Alsina, M. A.; Haro, I.; Reig, F.; Hudecz, F. Phospholipid-model membrane interactions with branched polypeptide conjugates of a hepatitis A virus peptide epitope. *Bioconjugate Chem.* **2000**, *11*, 30–38.

(35) Wimley, W. C.; White, S. H. Experimentally determined hydrophobicity scale for proteins at membrane interfaces. *Nat. Struct. Biol.* **1996**, *3*, 842–848.

(36) White, S. H.; Wimley, W. C. Hydrophobic interactions of peptides with membrane interfaces. *Biochim. Biophys. Acta* **1998**, *1376*, 339–352.

(37) Dathe, M.; Schumann, M.; Wieprecht, T.; Winkler, A.; Beyermann, M.; Krause, E.; Matsuzaki, K.; Murase, O.; Bienert, M. Peptide helicity and membrane surface charge modulate the balance of electrostatic and hydrophobic interactions with lipid bilayers and biological membranes. *Biochemistry* **1996**, *35*, 12612–12622.

(38) Wieprecht, T.; Dathe, M.; Schumann, M.; Krause, E.; Beyermann, M.; Bienert, M. Conformational and functional study of magainin 2 in model membrane environments using the new approach of systematic double-D-amino acid replacement. *Biochemistry* **1996**, *35*, 10844–10853.

(39) Van Mau, N.; Vie, V.; Chaloin, L.; Lesniewska, E.; Heitz, F.; Le Grimellec, C. Lipid-induced organization of a primary amphipathic peptide: a coupled AFM-monolayer study. *J. Membr. Biol.* **1999**, *167*, 241–249.

(40) Wender, P. A.; Mitchell, D. J.; Pattabiraman, K.; Pelkey, E. T.; Steinman, L.; Rothbard, J. B. The design, synthesis, and evaluation of molecules that enable or enhance cellular uptake: peptoid molecular transporters. *Proc. Natl. Acad. Sci. U.S.A.* **2000**, *97*, 13003–13008.

(41) Futaki, S.; Ohashi, W.; Suzuki, T.; Niwa, M.; Tanaka, S.; Ueda, K.; Harashima, H.; Sugiura, Y. Stearylated arginine-rich peptides: a new class of transfection systems. *Bioconjugate Chem.* **2001**, *12*, 1005–1011.

(42) Chen, L. L.; Frankel, A. D.; Harder, J. L.; Fawell, S.; Barsoum, J.; Pepinsky, B. Increased cellular uptake of the human immunodeficiency virus-1 Tat protein after modification with biotin. *Anal. Biochem.* **1995**, *227*, 168–175.

amino acid is at the interface that imparts surface activity to NPs and is available for interaction with lipid membrane.

The phase image of the EMM following interaction with $TAT_{200}$-RNPs shows complete condensation of EMM in comparison to the phase image of the EMM following interactions with RNPs (Figure 3b vs 3c). This observation is consistent with the analysis of the results from the Langmuir studies. TAT peptide facilitates NP interaction with the phospholipids of the model membrane and causes condensation of lipids, whereas RNPs come to the interface due to their surface active nature, but they do not interact with the EMM and hence do not cause condensation. Surface analysis of the LS films further confirms the penetration of TAT-RNPs into the EMM. This is clearly evident from the height analysis data of the NP-interacted EMM that showed significantly lower peaks for the TAT-conjugated NPs than for the unconjugated NPs and the average height is significantly lower than the TEM diameter of NPs (Figure 3f). Thus, it can be stated that the surface active property of NPs is essential for interaction to occur but it would not necessarily cause an interaction unless there is a hydrophobic chain at the interface to penetrate the membrane.

The greater uptake of ritonavir by HUVECs with TAT-RNPs could thus be attributed to the above biophysical interactions with cell lipid bilayer that could have facilated the internalization of NPs and hence drug delivery (Figure 4). In earlier study, we have reported greater uptake of ritonavir with TAT-conjugated RNPs in Madine Darby canine kidney cells overexpressing P-gp (MDCK-MDR1) than that with conjugated RNPs or drug in solution,[21] suggesting that the effect of TAT peptide on drug uptake does not seem depend upon the cell line. We have previously shown that the major fraction (98.5%) of NPs associated with cells is internalized, and hence the drug uptake determined above is primarily due to internalized NPs and not due to the cell surface associated NPs.[43]

In our recent study, we have determined the biophysical interactions of polystyrene NPs modified with different cationic surfactants. It was shown that the NPs which demonstrate greater biophysical interactions with a model membrane also demonstrate greater cellular uptake of NPs.[29] Despite the lack of all the characteristics of a typical cell membrane in a model membrane, such as the absence of anchoring membrane proteins, receptors, the bilayer lipid structure of cell membrane, and the active process of endocytosis, we found a good corelation between biophysical parameters and cellular uptake of the encapsulated therapeutics. Recently, we have shown that the force of adhesion of NPs with cell membrane plays a role cellular uptake of NPs.[3] Thus, it can be stated that the biophysical interactions of NPs with cell membrane play a significant role in triggering the process of intracellular uptake of nanocarriers.

It is interesting to note that NPs conjugated to a higher amount of TAT peptide ($TAT_{500}$-RNPs) demonstrated toxicity. These NPs showed an increase in SP of the EMM by 9 mN/m, whereas RNPs conjugated to a lower amount of peptide ($TAT_{200}$-RNPs), which did not show toxicity, caused an increase in SP of 6 mN/m (Table 1, Figure 5). This observation is tempting us to suggest that the NPs which show increase in SP beyond a certain value (<6 mN/m) could be toxic to cells. However, more studies with different types of NPs and cell lines would be required to support the above statement. It would be also interesting to know what changes in lipid arrangement cause toxicity.

Formulations of TAT-conjugated NPs have been extensively investigated for various applications including bioimaging, gene and drug delivery, and targeting.[44] Previously, we have demonstrated enhanced drug delivery to the brain with TAT-conjugated RNPs. These NPs were shown to cross the BBB and localize within the brain parenchyma.[21] Biophysical interactions with a model membrane thus could prove to be a useful technique in studying the effect of different CPPs and their sequence, designing of right peptide sequence for conjugation, and in optimizing the conjugation chemistry for the amount of peptide conjugated and its proper orientation, whereby contributing to the development of efficient nanocarrier systems for drug delivery applications.

## Conclusions

We have demonstrated that the TAT peptide sequence and the amount of it bound to the NP surface significantly influence the biophysical interactions of NPs with a model cell membrane. We have also shown that the biophysical interactions of NPs with the EMM correlate with cellular delivery of the encapsulated therapeutic agent, and hence could be effectively used in developing efficient nanocarrier systems for drug delivery applications.

**Acknowledgment.** The study reported here is funded by Grants 1R01 EB 003975 from the National Institute of Biomedical Imaging and Bioengineering and R21 MH06 7525 from the National Institute of Mental Health of the National Institutes of Health (to V.L.). K.S.R. is supported by a Predoctoral Fellowship from the American Heart Association, Heartland Affiliate (Grant No. 0710119Z). Authors thank Ms. Melissa Jedlicka for proofreading the manuscript.

**Supporting Information Available:** Additional experimental details as noted in text. This material is available free of charge via the Internet at http://pubs.acs.org.

MP900011H

(43) Qaddoumi, M. G.; Ueda, H.; Yang, J.; Davda, J.; Labhasetwar, V.; Lee, V. H. The characteristics and mechanisms of uptake of PLGA nanoparticles in rabbit conjunctival epithelial cell layers. *Pharm. Res.* **2004**, *21*, 641–648.

(44) Santra, S.; Yang, H.; Dutta, D.; Stanley, J. T.; Holloway, P. H.; Tan, W.; Moudgil, B. M.; Mericle, R. A. TAT conjugated, FITC doped silica nanoparticles for bioimaging applications. *Chem. Commun.* **2004**, 2810–2811.